

# An off-axis hydrothermal vent field near the Mid-Atlantic Ridge at 30° N

Deborah S. Kelley\*, Jeffrey A. Karson†, Donna K. Blackman‡, Gretchen L. Früh-Green§, David A. Butterfield\*||, Marvin D. Lilley\*, Eric J. Olson\*, Matthew O. Schrenk\*, Kevin K. Roell, Geoff T. Lebon||, Pete Rivizzigno† & the AT3-60 Shipboard Party

\* University of Washington, School of Oceanography, Seattle, Washington 98195, USA

† Duke University, Division of Earth & Ocean Sciences, Durham, North Carolina 27708-0230, USA

‡ Scripps Institution of Oceanography, La Jolla, California 92093-0225, USA

§ Institute For Mineralogy and Petrology, ETH-Zentrum, CH-8092, Zurich, Switzerland

|| Joint Institute for the Study of the Atmosphere & Ocean, University of Washington and NOAA Pacific Marine Environmental Laboratory, Seattle, Washington 98115, USA

**Evidence is growing that hydrothermal venting occurs not only along mid-ocean ridges but also on old regions of the oceanic crust away from spreading centres. Here we report the discovery of an extensive hydrothermal field at 30° N near the eastern intersection of the Mid-Atlantic Ridge and the Atlantis fracture zone. The vent field—named ‘Lost City’—is distinctly different from all other known sea-floor hydrothermal fields in that it is located on 1.5-Myr-old crust, nearly 15 km from the spreading axis, and may be driven by the heat of exothermic serpentinization reactions between sea water and mantle rocks. It is located on a dome-like massif and is dominated by steep-sided carbonate chimneys, rather than the sulphide structures typical of ‘black smoker’ hydrothermal fields. We found that vent fluids are relatively cool (40–75 °C) and alkaline (pH 9.0–9.8), supporting dense microbial communities that include anaerobic thermophiles. Because the geological characteristics of the Atlantis massif are similar to numerous areas of old crust along the Mid-Atlantic, Indian and Arctic ridges, these results indicate that a much larger portion of the oceanic crust may support hydrothermal activity and microbial life than previously thought.**

Most known hydrothermal fields along mid-ocean ridges are located on young crust where the cooling of hot basaltic material drives hydrothermal flow<sup>1</sup>. In such systems, precipitation of iron- and sulphide-rich minerals occurs during mixing of 200–400 °C hydrothermal fluids with cold, oxygenated sea water. The compositions of the resulting sulphide chimneys reflect fluid–rock reactions within the underlying basaltic–gabbroic substrate<sup>2,3</sup>. All evidence indicates that such black smoker systems and associated diffuse flow typify hydrothermal activity directly on-axis in mid-ocean-ridge environments. However, there is a growing body of evidence from recent water column and sea-floor studies indicating that lower-temperature venting associated with older, tectonized portions of the oceanic crust may be common along much of the mid-ocean-ridge spreading network<sup>4–6</sup>. Here we describe the Lost City hydrothermal field, which represents the first observation of this type of low-temperature venting associated with extensive chimney development. The Lost City field is spectacular in that it hosts numerous actively venting structures, one of which reaches 60 m in height. The steep-sided pinnacles are composed entirely of carbonate and magnesium hydroxide minerals, making them distinctly different from other well known mid-ocean-ridge hydrothermal vents.

## Geology and tectonic setting of the Lost City hydrothermal field

The Atlantis massif is located at the inside corner of the intersection of the Mid-Atlantic Ridge (MAR) and the 75-km, left-lateral offset, Atlantic transform fault (ATF) (Fig. 1)<sup>7,8</sup>. The massif is approximately 15 km across and the southern flanks are steep escarpments with 3,800 m of relief adjacent to the ATF. The upper surface of the dome is interpreted as a major low-angle normal or detachment fault<sup>7,8</sup> that has exposed variably metamorphosed peridotite and gabbro. The top of the scarp is marked by a sharply defined unconformity overlain by a laterally variable assemblage of very gently dipping, undeformed sedimentary rocks. These include carbonate cemented breccias with clasts of basalt, gabbro and peridotite, and well lithified, bedded carbonates. These are overlain by variably consolidated pelagic ooze with dispersed blocks and

rubble of basaltic and ultramafic material. The unconformity indicates that the southern end of the massif may have been near or even above sea-level before subsiding to its current depth of about 700 m. The south wall of the massif is a series of steep cliffs that define an extensive, south-facing embayment with several steep-sided ridges that extend southward toward the transform valley (Fig. 1). Magnetic anomaly patterns show that the centre of the massif, about 15 km west of the spreading axis, is about 1.5 Myr old, consistent with the local half-spreading rate of 12 mm yr<sup>-1</sup> (ref. 8).

## The Lost City field

Investigations of the southern wall of the massif, using the remotely operated imaging vehicle *ArgoII* and the submersible *Alvin*, resulted in the discovery of the Lost City field (LCF). The LCF rests on a terrace at a water depth of 700–800 m on a south-trending spur that protrudes from the crest of the south wall scarp (Fig. 1). The field is underlain by a diverse suite of mafic and ultramafic rocks that crop out on the cliffs immediately below the edge of the scarp. These include a complex assemblage of variably serpentinized and deformed peridotites, massive gabbro to oxide gabbro, and meta-gabbros. The hydrothermal structures and related deposits overlie and fill fractures in the capping carbonate unit and thus clearly post-date this assemblage. In addition, the vent structures lack pelagic sedimentary cover, suggesting that they may be relatively young.

Initial surveys of the surrounding area with *ArgoII* and *Alvin* indicate that the field extends for at least 400 m across the terrace and that it hosts at least 30 active and inactive structures (Fig. 2). To the south, cliff exposures have extensive areas of active and inactive white hydrothermal precipitates. These deposits fill fractures and form hundreds of shelf-like overhanging ledges or ‘flanges’ that protrude as much as 2 m from the cliff face.

Within the LCF, active and inactive vents exhibit a wide variety of morphologies that include small spires, mounds and pinnacles (Fig. 2a). The mounds are variably cemented, 10–20 m high, steep-sided deposits composed of small toppled spires that have been overgrown and cemented by hydrothermal precipitates. Larger

isolated pinnacles are commonly 10–30 m tall. But the most spectacular of the pinnacles is a giant columnar tower that rises 60 m above the sea floor, making it the tallest hydrothermal deposit yet discovered anywhere on the sea floor. The top of this composite structure is 15 m across and hosts four smaller spires. At least one of these spires is actively venting 75 °C fluid from its top. On this and other large pinnacles, flanges exhibit concave-down forms, which trap highly reflective pools of 40–55 °C vent fluid (Fig. 2b). Delicate fingers and dendritic growth ornament the edges and tops of the flanges; stalagmite-like cones rise several metres from the tops of some flanges. In most cases, fresh-looking white deposits indicate

that active venting occurs on the tops of the spires and pinnacles as well as from the flanges.

### Mineral and fluid chemistry

X-ray diffraction analyses of samples from seven inactive and active chimneys and flanges indicate that the structures are composed of variable mixtures of calcite ( $\text{CaCO}_3$ ), aragonite ( $\text{CaCO}_3$ ), and brucite ( $\text{Mg}(\text{OH})_2$ ). The composition of the structures is reflected in the chemistry of three vent fluid samples collected with *Alvin* from a 40 °C and 75 °C site. The pH of the vent fluids measured at 25 °C is high (9.0 to 9.8 versus 8.0 for ambient sea water) (Table 1).

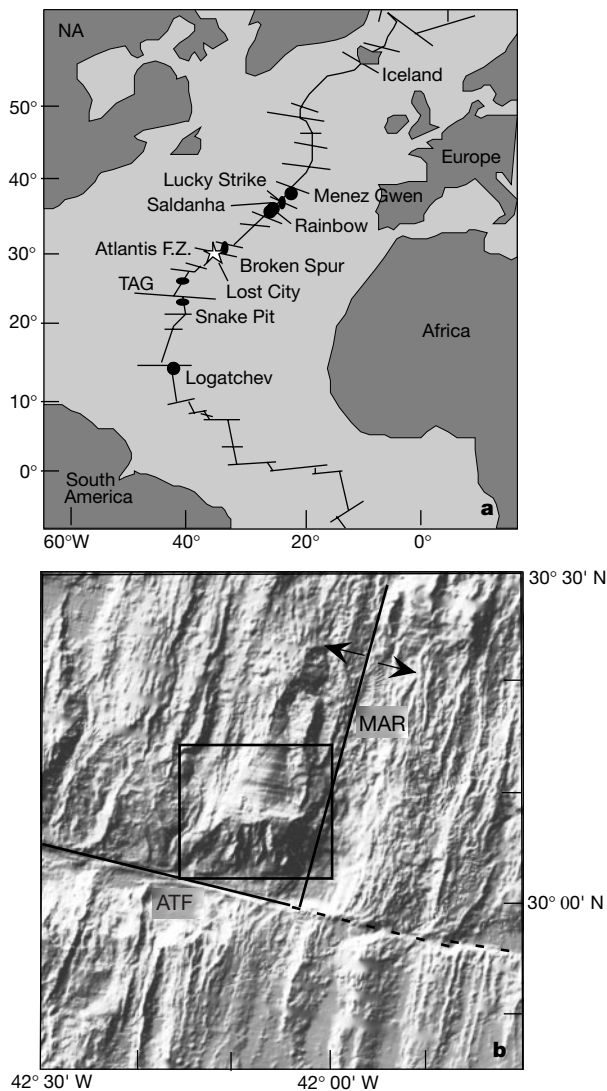


**Figure 1** The Mid-Atlantic Ridge and location of the Lost City field. **a**, Location of active hydrothermal sites along the Mid-Atlantic Ridge (dots) and the Lost City hydrothermal field on the Atlantis massif at 30° N. In addition to the Lost City, the Logatchev, Rainbow and Saldanha fields are also hosted on peridotite and gabbroic material. Saldanha most closely resembles the LCF in that it is also located on a peridotite massif at a water depth of 700 m, it hosts filamentous bacteria, and no vent fauna were identified. Venting of clear, warm fluids was observed from small orifices through sediment<sup>6</sup>. **b**, Shaded relief map showing the location of the Atlantic massif and the study site (box). Also shown is the location of the Mid-Atlantic Ridge (MAR) and the Atlantis transform fault (ATF). The southern face of the massif is a steep sided scarp with nearly 3,800 m of relief. The hydrothermal field is located at a water depth of about 700 m near the top of the massif. The dotted line denotes the trace of the ATF.

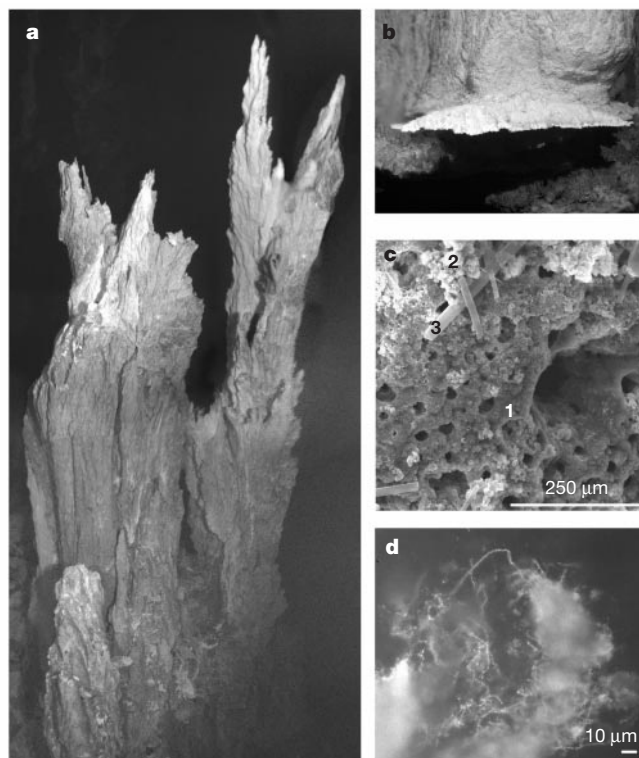


**Figure 2** Hydrothermal deposits and microbial communities within the Lost City field. **a**, Photomosaic of an inactive 8-m-tall carbonate chimney in the eastern portion of the Lost City field. This mosaic was produced from digital still camera imagery collected every 15 s by the remotely operated vehicle *ArgoII*. The calcite, aragonite and brucite chimneys form delicate to massive pinnacles that reach up to 60 m in height. **b**, Aragonite and brucite flange venting 40 °C fluids (shimmering water in left portion of the image). The carbonate ledges grow horizontally out from the chimney walls and trap buoyant reflecting pools of warm water, which seeps out from the main structure walls. Mixing of sea water and diffusely venting fluids that spill out upward over the lip of the flanges, and up through porous flange tops results in outward growth and thickening of the flanges. The flange shown in this image is about 1 m in width and hosts abundant microbial communities. **c**, Scanning electron image (SEM) of a piece of the flange shown in **b**, collected with *Alvin*. Elemental detection and X-ray diffraction analyses of this sample show that it contains a fine porous matrix of calcium carbonate (aragonite) (point 1), and magnesium hydroxide ( $\text{Mg}(\text{OH})_2$ ) minerals (points 2 and 3), which exhibit variable morphologies. The SEM used was an ISI DS-130s with an operating voltage of 18 kV. The images were collected using ITRF Iridium II EDS software. Molecular ratios were determined using ZAF (atomic number, absorption, fluorescence) corrections after deconvolution through the ITRF software. Specimens were sputter coated with palladium before being analysed. **d**, Epifluorescent microphotograph of DAPI (4',6-diamidino-2-phenylindole)-stained filamentous microbial communities in the flange sample collected from the site shown in **b**. Continuous biofilms composed of several types of microbial cells were observed attached to mineral surfaces within the active vent structures. Microbial cells ranged from 0.5 to 2.0  $\mu\text{m}$  in diameter and included cocci, rods and filaments. Significant biomass is observed within the active samples recovered.

These values are in marked contrast to vent fluids collected from basalt-hosted environments where pH values measured at 25 °C are typically 3.0 to 5.0 (Table 1). High pH and Ca concentration are typical of fluids emanating from serpentinized ultramafic rocks<sup>9,10</sup> and promote carbonate precipitation upon mixing with sea water.

Lost City fluids have magnesium concentrations much lower than sea water (9–19 mmol kg<sup>-1</sup> versus 54 mmol kg<sup>-1</sup>) and the three samples show nearly linear mixing trends when other major elements are plotted against Mg. As there is brucite in the chimneys and flanges, Mg is probably reactive within the edifices. Mg<sup>2+</sup> activity derived from sea water in the fluids may favour the precipitation of aragonite, which is present in many of the Lost City samples and is commonly found associated with serpentinized peridotites<sup>11–15</sup>. Ca is enriched more than twofold in the fluids, but K is within 3% of the ambient seawater value. The 75 °C fluids have slightly higher Ca concentration at zero Mg than the cooler samples, consistent with progressive seawater mixing and carbonate precipitation. Reactive silicate (measured after two weeks of refrigerated storage) is lower than ambient sea water in the 40 °C samples, but is slightly higher than sea water in the 75 °C sample. Silica is a trace component within the chimney minerals. Over 60 μmol kg<sup>-1</sup> of total H<sub>2</sub>S was detected after nine days of sample storage, and SO<sub>4</sub> is in excess over values predicted from mixing sea water and an upwelling end-member with zero Mg and SO<sub>4</sub>. Na and Cl are both within 1% of the sea-water value (Table 1). Measured hydrogen and methane concentrations were 249–428 and 136–285 mmol kg<sup>-1</sup>, respectively.

The LCF is the first known example of sea-floor vents capable of producing the low Mn/CH<sub>4</sub> plumes that are common along fracture zones and non-transform offsets of the MAR. The high Ca, low Mg and near-ambient silica content are consistent with peridotite-dominated fluid–rock interaction<sup>16,17</sup> producing an alkaline fluid that precipitates carbonates and hydroxides below the sea floor and upon mixing with sea water.

Interaction of mantle materials with sea water during serpentinization is further supported by stable isotope analyses of carbonate in the pinnacle structures. For the seven samples recovered, the δ<sup>13</sup>C values range from 1.0 to 2.1‰ (VPDB, the Vienna Pee Dee belemnite standard) and clearly reflect a marine source of

carbon<sup>14</sup>. The δ<sup>18</sup>O values of 32.5 to 35.4‰ (VSMOW, Vienna Standard Mean Ocean Water) are slightly enriched in <sup>18</sup>O relative to marine carbonates, but they are typical values for aragonite associated with oceanic serpentinites (31–36‰ VSMOW)<sup>12,14,15</sup>. Calculations based on published oxygen isotope fractionation factors and a temperature of 7 °C (as measured for the ambient bottom water in the area) indicate that most of the pinnacle and flange carbonates were precipitated from altered sea water with δ<sup>18</sup>O values of 0.5 to 2‰ (VSMOW). These values are consistent with δ<sup>18</sup>O values of serpentinizing fluids calculated from serpentine oxygen isotope data from different tectonic environments<sup>13–15</sup> and suggest that active subsurface serpentinization reactions below the massif control the oxygen isotope signatures of the fluids venting in the LCF.

### Life within the vent system

Within this field, the active carbonate chimneys are typically awash in buoyantly rising mixtures of warm shimmering vent fluid and cooler sea water. These diffusely venting areas support dense microbial communities that commonly form white to light grey coloured filamentous strands several centimetres in length. Preliminary investigations of microbial communities show extensive biofilm development on mineral surfaces within the carbonate structures (Fig. 2d). Samples obtained from a 75 °C site at the top of the 60-m-tall structure contain abundant biomass, which exists primarily as microcolonies and isolated cells on the surfaces of carbonate minerals (Fig. 2d). Enrichment culturing of chimney material in aerobic and anaerobic media yielded microorganisms in the thermophilic (50 °C, 70 °C) and mesophilic (25 °C) temperature regimes. Preliminary results of DNA extraction and analysis from recovered flange and chimney material indicates that Archaeal and Eubacterial lineages are both present at Lost City. However, macrofaunal assemblages that typify most vent environments<sup>18</sup> are extremely rare within the LCF and are limited to a few crabs, sea urchins, and abundant sponges and corals.

### Global significance of off-axis venting

During the past two decades hydrothermal fields have been explored at over 40 sites along the mid-ocean-ridge spreading network<sup>1,6,19–21</sup>. Eight of these occur along the axis of the MAR and three are hosted

**Table 1 Summary of vent fluid data**

| Location               | Host rock           | T (°C)  | pH        | Mg (mmol kg <sup>-1</sup> ) | Ca (mmol kg <sup>-1</sup> ) | Na (mmol kg <sup>-1</sup> ) | Cl (mmol kg <sup>-1</sup> ) | SO <sub>4</sub> (mmol kg <sup>-1</sup> ) | H <sub>2</sub> S (mmol kg <sup>-1</sup> ) | CH <sub>4</sub> (mmol kg <sup>-1</sup> ) | H <sub>2</sub> (mmol kg <sup>-1</sup> ) | Reference |
|------------------------|---------------------|---------|-----------|-----------------------------|-----------------------------|-----------------------------|-----------------------------|--|---|--|---|-----------|
| Sea water              |                     | 7       | 8.0       | 54.0                        | 10.4                        | 475                         | 553                         | 28.6                                     | 0   | 4 × 10 <sup>-7</sup>                     | 4 × 10 <sup>-4</sup>                    |           |
| Lost City; 30° N MAR   | Peridotite + gabbro | 40–75   | 9–9.8     | 9–19                        | 21.0–23.3                   | 479–485                     | 546–549                     | 5.9–12.9                                 | 0.064                                     | 0.13–0.28                                | 0.25–0.43                               | This work |
| Rainbow; 36° 14' N     | Peridotite + gabbro | 360     | 2.9–3.1   |                             |                             |                             | >750                        |  | <2.5                                      | 2.2                                      | 13.0                                    | 19        |
| Broken Spur; 29° N MAR | Basalt              | 356–360 |           | 0                           | 11.8–12.8                   | 419–422                     | 469                         |  | 9.30                                      | 0.06                                     | 0.43                                    | 38        |
| Lucky Strike;          | Basalt              | 308–324 | 3.8–6.4   | 0                           | 32.3–36.7                   | 347–426                     | 417–472                     |  | 2.1–3.0                                   | 0.3–0.7                                  | 0.04–0.72                               | 20        |
| 37° 17' N MAR          |                     | 185–284 | 3.8–3.9   | 0                           | 31.3–38.2                   | 363–428                     | 424–514                     |  | 2.0–3.0                                   | 0.4–0.8                                  | 0.003–0.27                              |           |
| Menez Gwen;            | Basalt              | 275–284 | 4.2–4.8   | 0                           | 29.7–33.1                   | 312–319                     | 357–381                     |  | 1.3–1.8                                   | 1.5–2.1                                  | 0.02–0.05                               | 20        |
| 37° 50' N MAR          |                     |         |           |                             |                             |                             |                             |  |   |  |   |           |
| Conical seamount†      | Peridotite          | 3       | 9.28      |                             |                             |                             |                             | 30–40                                    | 2.1                                       | 0.001                                    |   | 11, 12    |
| Endeavour, JdF‡        | Basalt              | 346–370 | 4.2–4.5   | 0                           | 13.8–42.9                   | 260–391                     | 350–370                     | 0–2                                      | 3.0–8.1                                   | 1.8–3.4                                  | 0.16–0.42                               | 39–41     |
| 21° N EPR              | Basalt              | 273–355 | 3.3–3.8   | 0                           | 11.7–20.8                   | 432–510                     | 489–579                     | 0–0.6                                    | 6.6–8.4                                   | 0.06–0.09                                | 0.23–1.7                                | 40, 41    |
| Oman Ophiolite§        | Peridotite          | 23      | 11.4–11.6 | 0.002–0.01                  | 1.5–1.9                     | 11.5–35.9                   | 9.67–26.1                   | 0.05–0.14                                |   |  |   | 42        |
| Experiments            |                     |         |           |                             |                             |                             |                             |  |   |  |   |           |
|                        | Harzburgite         | 300     | 6.4–11.6  | 0.002–0.02                  | 0.29–5.24                   | 549–576                     | 512–541                     | 12.1–17.8                                | 0.6–0.8                                   | 0.066                                    | 0.10–0.33                               | 16        |
|                        | Lherzollite         | 200     | 5.4–8.0   | 10.7–49.4                   | 7.5–35.7                    | 467–500                     | 534–560                     | 2.04–24.8                                | ND  | ND                                       | ND                                      | 16        |
|                        | Basalt              | 350     | 4.8       | 0.050                       | 18.3                        | 492                         | 581                         | 0.069                                    | 7.3                                       | 1.0                                      | 0.2                                     | 43        |
| Theoretical            | Peridotite          | 350     | 6.5–6.6   | 0.07–0.1                    | 27.6–35.6                   | 471–543                     | 550–612                     | <<1.0                                    | 3.2–6.3                                   |  | 20.96–164.9                             | 17        |

Fluids were sampled in titanium, non gas-tight samplers with *Alvin*. Ten millilitres of fluid was drawn into 20-ml syringes and 10-ml headspace air was added. The samples were immediately frozen at -70 °C to halt biological oxidation of gas species. Methane and H<sub>2</sub> values for Lost City are a minimum as gases were probably lost during sampling and/or diffusively during storage. H<sub>2</sub>S concentrations are also minimum values because samples were not run onboard, but after ~2 weeks in cold storage. It is therefore likely that oxidation occurred. MAR, Mid-Atlantic Ridge; JdF, Juan de Fuca ridge; EPR, East Pacific Rise; ND, not detectable.

† Conical seamount is located in the Mariana forearc and contains sedimentary serpentine. It was drilled during Leg 125 of the Ocean Drilling Program. Trace element and stable isotopic compositions of carbonate chimney samples and serpentinized matrix material has been interpreted to reflect fluids with either a forearc mantle or subducted slab component, or both<sup>12</sup>.

‡ Carbon isotopic values of δ<sup>13</sup>C in CH<sub>4</sub> of -55‰ in the Endeavour fluids are interpreted to indicate a microbial source for the methane<sup>40</sup>.

§ Meteorite fed springs emanate from serpentinized harzburgite. The spring waters are oversaturated with respect to both serpentine and brucite. Mixing of bicarbonate-rich fluids and surface water results in precipitation of calcite or aragonite.

|| This experimental work involved reaction of harzburgitic material and an Mg-free solution at 300 °C, 500 bar, and a water-rock ratio of 10. The harzburgitic runs lasted 0–17,147 hours; additional experiments included reacting lherzollite with sea water at 200 °C, 500 bar and at water-rock ratio of 10 for 0–4,869 h.

by serpentinized peridotites (Fig. 1b). Few data are published on these three sites, but both the Rainbow and Logatchev sites host black smoker chimneys (350–360 °C)<sup>19–22</sup>. High CH<sub>4</sub> and H<sub>2</sub> concentrations at these two sites indicate a peridotite influence; however, much of the chemical data (low pH values, moderate silica, Cu and Zn enrichment) are consistent with reactions involving gabbroic or basaltic material<sup>19,22,23</sup>.

Recent studies suggest that hydrothermal systems similar to the LCF may be common along a significant portion of the ridge system (for example, the MAR, and the Indian and Arctic ridges). The sea-floor morphology in the vicinity of the ATF is typical of that near many large transform faults that offset the MAR and Southern Ocean ridges<sup>4–7</sup>. Serpentinite bodies routinely crop out at these sites and the recovered peridotites are typically pervasively altered to serpentine minerals, indicating extensive interaction with hydrothermal fluids<sup>14,21,24</sup>. Serpentinization processes have been the focus of much attention of late because of their potential importance to early Earth hydrothermal systems and because they generate significant CH<sub>4</sub>, H<sub>2</sub> and possibly organic compounds during mineral–fluid reactions<sup>25–29</sup>. Manifestation of such reactions is commonly inferred from CH<sub>4</sub> and H<sub>2</sub> anomalies in the water column at numerous uplifted serpentinite massifs, at highly tectonized zones believed to be peridotitic in composition, and at serpentinite outcrops along rift valley walls<sup>4–6,9,30–33</sup>. A significant number of these venting sites are located on old, highly tectonized crust away from the neovolcanic zone<sup>4,5</sup>. The extensive nature of these plumes suggests that such venting may play a significant role in chemical and thermal exchanges between the upper mantle and the lithosphere<sup>4,5,9</sup>. However, except for the Saldanha field at 36° 30' N, located near the southern tip of the FAMOUS segment<sup>6</sup>, few of these sites have ever been visited.

There are many features of slow- and ultraslow-spreading systems which favour venting from off-axis environments. For example, tectonic emplacement of inside corner highs, faulting associated with transform displacements, isostatic uplift, and exfoliation induced by mass wasting probably create permeable pathways in the serpentinite basement. Within these environments, the combination of exothermic serpentinization reactions, active fracturing, and topographic forcing may drive fluid flow. Compressive stresses may also be generated on steep scarps due to the large positive volume changes (~20%) associated with serpentinization reactions. In concert, these factors promote low-temperature venting of high-pH, methane- and hydrogen-rich fluids in hydrothermal systems associated with uplifted, ultramafic massifs that are common along slow- and ultraslow-spreading ridges.

### Implications for biology and early Earth hydrothermal systems

We anticipate that this newly discovered class of sea-floor hydrothermal system may provide insights into hydrothermal processes of the early Earth and the life forms that they supported<sup>25,34</sup>. The reducing conditions associated with serpentinization of ultramafic material may be similar to those present in the Hadean (4.5–3.8 Gyr ago) ocean during early Earth formation and it has been suggested that such high-pH systems may have been a requirement for the emergence of life on the ocean floor<sup>25,35,36</sup>. Model calculations based on thermodynamic considerations suggest that synthesis of numerous organic compounds is favoured during mixing of warm serpentinite-derived, high-pH, reducing fluids with cool, oxygenated sea water<sup>25</sup>. The warm, organic- and volatile-rich environment present within the porous interior of ancient hydrothermal deposits may have been extremely suitable habitats for the emergence of thermophilic or hyperthermophilic anaerobic organisms that may represent the most ancient of lifeforms on Earth<sup>37</sup>.

The LCF is an example of a previously unknown type of sea-floor chemosynthetic system that may be much more widespread than the highly localized, magmatically driven hydrothermal vent systems present along mid-ocean-ridge axes. It is a reminder of the

discoveries remaining to be made on the sea floor, which may hold important clues to the origin and diversity of life. □

Received 16 February; accepted 6 June 2001.

- Fornari, D. J. & Embley, R. W. in *Seafloor Hydrothermal Systems, Physical, Chemical, Biological, and Geological Interactions* (eds Humphris, S. E., Zierenberg, R. A., Mullineaux, S. & Thomson, R. E.) 1–26 (American Geophysical Union Monograph 91, Washington DC, 1995).
- Hannington, M. D., Jonasson, I. R., Herzig, P. M. & Petersen, S. in *Seafloor Hydrothermal Systems, Physical, Chemical, Biological, and Geological Interactions* (eds Humphris, S. E., Zierenberg, R. A., Mullineaux, S. & Thomson, R. E.) 115–157 (American Geophysical Union Monograph 91, Washington DC, 1995).
- Tivey, M. K., Stakes, D. S., Cook, T. L., Hannington, M. D. & Petersen, S. A model for growth of steep-sided vent structures on the Endeavour Segment of the Juan de Fuca Ridge: Results of a petrologic and geochemical study. *J. Geophys. Res.* **104**, 22859–22883 (1999).
- German, C. R., Parson, L. M. & HEAT Scientific Team. Hydrothermal exploration near the Azores Triple Junction: tectonic control of venting at slow-spreading ridges? *Earth Planet. Sci. Lett.* **138**, 93–104 (1996).
- Gracia, E., Charlou, J. C., Radford-Knoery, J. & Parson, L. M. Non-transform offsets along the Mid-Atlantic Ridge south of the Azores (38°N–34°N): ultramafic exposures and hosting of hydrothermal vents. *Earth Planet. Sci. Lett.* **177**, 89–103 (2000).
- Barriga, F. J. A. S. et al. Discovery of the Saldanha Hydrothermal field on the FAMOUS Segment of the MAR (36° 30' N). *Eos* **79**, 67 (1998).
- Cann, J. R. et al. Corrugated slip surfaces formed at ridge-transform intersections on the Mid-Atlantic Ridge. *Nature* **385**, 329–332 (1997).
- Blackman, D. K., Cann, J. R., Janes, B. & Smith, D. K. Origin of extensional core complexes: Evidence from the Mid-Atlantic Ridge at Atlantis Fracture Zone. *J. Geophys. Res.* **103**, 21315–21333 (1998).
- Coleman, R. G. Petrologic and geophysical nature of serpentinites. *Geol. Soc. Am. Bull.* **82**, 897–918 (1971).
- Barnes, L., Rapp, J. R., O'Neil, J. R., Sheppard, R. A. & Gude, A. J. Metamorphic assemblages and the direction of flow of metamorphic fluids in four instances of serpentinization. *Contrib. Mineral. Petrol.* **35**, 263–276 (1972).
- Fryer, P. et al. Conical Seamount: SeamarCII, ALVIN submersible and seismic reflection studies. *Proc. ODP Init. Rep.* **125**, 69–94 (1990).
- Haggerty, J. A. in *Seamounts, Islands, and Atolls* (eds Keating, B., Fryer, P. & Batiza, R.) 175–185 (American Geophysical Monograph Series 47, Washington DC, 1987).
- Bonatti, E., Lawrence, J. R., Hamlyn, P. R. & Breger, D. Aragonite from deep sea ultramafic rocks. *Geochim. Cosmochim. Acta* **44**, 1207–1214 (1980).
- Früh-Green, G. L., Pias, A. & Lecuyer, C. Petrologic and stable isotope constraints on hydrothermal alteration and serpentinization of the EPR shallow mantle at Hess Deep (Site 895). *Proc. ODP Sci. Res.* **147**, 255–291 (1996).
- Sakai, R., Kusakabe, M., Noto, M. & Ishii, T. Origin of waters responsible for serpentinization of the Izu-Ogasawara-Mariana forearc seamounts in view of hydrogen and oxygen isotope ratios. *Earth Planet. Sci. Lett.* **100**, 291–303 (1990).
- Janecky, D. R. & Seyfried, W. E. Jr Hydrothermal serpentinization of peridotite within the oceanic crust: Experimental investigations of mineralogy and major element chemistry. *Geochim. Cosmochim. Acta* **50**, 1357–1378 (1986).
- Wetzel, L. R. & Shock, E. L. Distinguishing ultramafic from basalt-hosted submarine hydrothermal systems by comparing calculated vent fluid compositions. *J. Geophys. Res.* **105**, 8319–8340 (2000).
- Van Dover, C. L. in *The Ecology of Deep-Sea Hydrothermal Vents* 63–69 (Princeton Univ. Press, Princeton, New Jersey, 2000).
- Donval, J. P. et al. High H<sub>2</sub> and CH<sub>4</sub> content in hydrothermal fluids from Rainbow site newly sampled at 36° 14' N on the AMAR segment, Mid-Atlantic Ridge (diving FLORES cruise, July 1997). Comparison with other MAR sites. *Eos* **78**, 832 (1997).
- Charlou, J. L. et al. Compared geochemical signatures and the evolution of Menez Gwen (37° 50' N) and Lucky Strike (37° 17' N) hydrothermal fluids, south of the Azores Triple Junction on the Mid-Atlantic Ridge. *Chem. Geol.* **171**, 49–75 (2000).
- Krasnov, S. G. et al. in *Hydrothermal Vents and Processes* (eds Parson, L. M., Walker, C. L. & Dixon, D. R.) 43–64 (Geological Society Special Publication 87, London, 1995).
- Douville, E., Charlou, J. L., Donval, J. P., Knoery, J. & Fouquet, Y. Trace elements in fluids from the new Rainbow hydrothermal field (36° 14' N, MAR): a comparison with other Mid-Atlantic Ridge fluids. *Eos* **78**, 832 (1997).
- Fouquet, Y. Geological setting and compositions of hydrothermal sulfide deposits along the Mid-Atlantic Ridge. Volcanic control versus tectonic control of sulfide mineralization. *Eos* **78**, 832 (1997).
- Lagabrielle, Y. D., Bideau, D., Cannat, M., Karson, J. A. & Mevel, C. in *Faulting and Magnetism at Mid-Ocean Ridges* (eds Buck, W. R., Delaney, P. T., Karson, J. A. & Lagabrielle, Y.) 153–176 (American Geophysical Union Monograph 106, Washington, DC, 1998).
- Shock, E. L. & Schulte, M. D. Organic synthesis during fluid mixing in hydrothermal systems. *J. Geophys. Res.* **103**, 28513–28527 (1998).
- Allen, D. A., Berndt, M. E., Seyfried, W. E. Jr & Horita, J. Inorganic reduction of CO<sub>2</sub> to HCOOH, CH<sub>4</sub>, and other reduced carbon compounds with application to seafloor hydrothermal systems. *Eos* **79**, 58–59 (1998).
- Berndt, M. E., Allen, D. E. & Seyfried, W. E. Jr Reduction of CO<sub>2</sub> during serpentinization of olivine at 300 °C and 500 bar. *Geology* **24**, 351–354 (1996).
- Janecky, D. R. & Seyfried, W. E. Jr Hydrothermal serpentinization of peridotite within the oceanic crust: Experimental investigations of mineralogy and major element chemistry. *Geochim. Cosmochim. Acta* **50**, 1357–1378 (1986).
- Neal, C. & Stanger, G. Hydrogen generation from mantle source rocks in Oman. *Earth Planet. Sci. Lett.* **66**, 315–320 (1983).
- Karson, J. A. & Lawrence, R. M. Tectonic setting of serpentinite exposures on the western median valley wall of the MARK area in the vicinity of Site 920. *Proc. ODP Sci. Res.* **153**, 5–21 (1997).
- Rona, P. A. et al. Hydrothermal circulation, serpentinization and degassing at a rift-valley fracture zone intersection: Mid-Atlantic Ridge near 15° N, 45° W. *Geology* **20**, 783–786 (1992).

32. Charlou, J. L. *et al.* Intense CH<sub>4</sub> degassing generated by serpentinization of ultramafic rocks at the intersection of the 15°20' N fracture zone and the Mid-Atlantic Ridge. *Geochim. Cosmochim. Acta* **62**, 2323–2333 (1998).
33. Bougault, H. *et al.* FAMOUS and AMAR segments on the Mid-Atlantic Ridge: ubiquitous hydrothermal Mn, CH<sub>4</sub>, δ<sup>3</sup>He signals along the rift valley walls and rift offsets. *Earth Planet. Sci. Lett.* **161**, 1–17 (1998).
34. Schopf, J. W. *Earth's Earliest Biosphere: Its Origin and Evolution* (ed. Schopf, J. W.) 1–543 (Princeton Univ. Press, New Jersey, 1983).
35. Russell, M. J. & Hall, J. A. The emergence of life from iron monosulfide bubbles at a submarine hydrothermal redox and pH front. *J. Geol. Soc. Lond.* **153**, 1–26 (1996).
36. MacLeod, G., McKeown, C., Hall, H. J. & Russell, M. J. Hydrothermal and oceanic pH conditions of possible relevance to the origin of life. *Orig. Life Evol. Biosph.* **23**, 19–41 (1994).
37. Pace, N. R. A molecular view of microbial diversity and the biosphere. *Science* **276**, 734–740 (1997).
38. James, R. H., Elderfield, H. & Palmer, M. R. The chemistry of hydrothermal fluids from the Broken Spur site, 29° N Mid-Atlantic Ridge. *Geochim. Cosmochim. Acta* **59**, 651–659 (1995).
39. Butterfield, D. A. *et al.* Gradients in the composition of hydrothermal fluids from Endeavour Ridge vent field: Phase separation and brine loss. *J. Geophys. Res.* **99**, 9561–9583 (1994).
40. Lilley, M. D. *et al.* Anomalous CH<sub>4</sub> and NH<sub>4</sub><sup>+</sup> concentrations at an unsedimented mid-ocean ridge hydrothermal system. *Nature* **364**, 45–47 (1993).
41. Von Damm, K. L. in *Seafloor Hydrothermal Systems: Physical, Chemical, Biological, and Geological Interactions* (eds Humphris, S. E., Zierenberg, R. A., Mullineaux, S. & Thomson, R. E.) 222–247 (American Geophysical Union Geophysical Monograph 91, Washington DC, 1995).
42. Neal, C. & Stanger, G. Calcium and magnesium hydroxide precipitation from alkaline groundwaters in Oman, and their significance to the process of serpentinization. *Mineral. Mag.* **48**, 237–241 (1984).
43. Seewald, J. S. & Seyfried, W. E. Jr The effect of temperature on metal mobility in subseafloor hydrothermal systems: Constraints from basalt alteration experiments. *Earth Planet. Sci. Lett.* **101**, 388–403 (1990).

### Acknowledgements

Shipboard party participants on cruise AT03-60 include N. Bacher, M. Basgall, D. K. Blackman, J. Cann, G. L. Frith-Green, J. S. Gee, H. Hanna, S. D. Hurst, B. E. John, J. A. Karson, D. S. Kelley, S. Lyons, J. Morgan, S. Nooner, P. Rivizzigno, D. K. Ross, G. Sasagawa and T. Schroeder. We thank the pilots, officers and crew of the RV *Atlantis-Alvin* for their professional service during this cruise. We are also grateful to the operators of *ArgoII* for their expert navigation of the camera system during the discovery exploration dive to this field. We also thank P. Hickey for piloting of *Alvin*, his sampling and his observation during the submersible dive. Support for this program was provided by the National Science Foundation.

Correspondence and requests for materials should be addressed to D.S.K. (e-mail: kelley@ocean.washington.edu).